Bulletin of Earthquake Engineering (2019) 17:2093–2113
https://doi.org/10.1007/s10518-018-00534-8

ORIGINAL RESEARCH

Estimating seismic demands of singly symmetric buildings by spectrum-based pushover analysis

Yang Liu[1] · **J. S. Kuang**[1]

Received: 2 June 2018 / Accepted: 3 December 2018 / Published online: 10 December 2018
© Springer Nature B.V. 2018

Abstract

Buildings with the singly symmetric plan are more vulnerable to earthquake actions than the buildings with a symmetric-plan arrangement since the torsional effect caused by the asymmetricity will induce higher seismic demand and may cause unexpected damage to the buildings. Thus, it is a crucial challenge for researchers and engineers to predict seismic demands of asymmetric-plan buildings for the possible strengthening and retrofitting. Although some pushover-based analysis methods have been proposed for the fast prediction of asymmetric-plan buildings, most of them do not reasonably consider the dynamic coupling of vibration modes. This paper expands the spectrum-based pushover analysis (SPA) procedure, which is proved to be effective in predicting seismic demands of buildings with symmetric building plans, to three-dimensional structure systems, to estimate the seismic demands of singly symmetric structures. A comprehensive case study, which includes six frame buildings with different structural heights and mass eccentricity ratios under various levels of the input motions, was conducted to investigate the feasibility of the SPA method in estimating the seismic demands of one-way asymmetric-plan buildings. It is found from the comparison of seismic demands computed from the SPA method, the nonlinear response time history analysis, the consecutive modal pushover analysis and the modal pushover analysis that the SPA method is capable of predicting the seismic demands very well, in particular, the demands on the heavy side of the structure, where the seismic demand and damage are more significant.

Keywords Spectrum-based pushover analysis · Singly symmetric building · Seismic demand Torsional effect · Dynamic coupling of vibration modes

1 Introduction

In high seismicity regions, such as Chile and Japan, most buildings were designed with symmetric plans to avoid the serious torsional effect, which will cause unexpected damage to buildings under seismic actions. However, in regions with moderate and

✉ J. S. Kuang
cejkuang@ust.hk

1 Department of Civil and Environmental Engineering, The Hong Kong University of Science and Technology, Kowloon, Hong Kong, China

low seismic activity, where non-seismic design philosophy is generally adopted in the design of structures, buildings with asymmetric plans are very popular to achieve attractive architectural appearance. The non-seismic designed buildings are inherently vulnerable to earthquake attacks, and the torsional effect induced by the asymmetric building plans will make those non-seismically designed structures even more dangerous when an earthquake happens. Hence, there is an urgent need for researchers and engineers to quickly estimate the seismic demand of the non-seismically designed structures with asymmetric-plan buildings.

During the past two decades, impressive progress has been achieved in the development of the fast prediction for seismic demands of buildings structures, and different pushover-based analysis methods are developed for estimating the seismic demand of buildings with symmetric and asymmetric plan arrangements (Antoniou et al. 2002; Antoniou and Pinho 2004a, b; Chopra and Goel 2004; Chopra et al. 2004; Poursha et al. 2009, 2011, 2014; Reyes and Chopra 2011a, b; Khoshnoudian and Kiani 2012; Kreslin and Fajfar 2012; Shakeri et al. 2012; Bhatt and Bento 2014; Brozovič and Dolšek 2014; Bergami et al. 2017; Liu and Kuang 2017). By including the torsional moment in forces and computing the seismic demand of vibration modes separately, the modal pushover analysis (MPA) method (Chopra and Goel 2002, 2004; Reyes and Chopra 2011a, b) was extended to three-dimensional cases to conduct a seismic analysis of asymmetric buildings. Similarly, the extended N2 method (Kreslin and Fajfar 2012) considers separately the seismic demand of different vibration modes of asymmetric structures. In the extended N2 method, a linear elastic response spectrum analysis procedure is combined with the conventional N2 method and the seismic demand from the extended N2 is the maximum demand of the conventional N2; then the demand of the linear response spectrum analysis procedure is amplified by an amplification factor. On the other hand, consecutive modal pushover analysis (CMP) methods (Poursha et al. 2011; Khoshnoudian and Kiani 2012) do not consider that the seismic demand of different vibration modes of asymmetric structures is independent. All these advanced pushover methods can provide a rational prediction of seismic demand of the buildings with asymmetric plans, but they all do not deal with the mode coupling in the analysis of the nonlinear seismic behaviour of the structures properly. However, since the mode coupling effect has a significant effect on the structural nonlinear seismic response, ignoring the coupling effects will induce errors in the seismic demand prediction.

The objective of this study is to expand the spectrum-based pushover analysis (SPA) procedure (Liu and Kuang 2017), which is originally developed for two-dimensional structures, to three-dimensional structure systems for quickly predicting the seismic demand of singly symmetric buildings. The simplification of the mode coupling, which is proved to be effective in calculating the seismic demand of buildings with a symmetric plan, is adopted for the proper consideration of mode coupling effect in the seismic analysis of buildings with asymmetric plans. Two series of steel moment-resisting frames, which have various heights and mass eccentricities and were subjected to different input motion levels, were studied to verify the feasibility of the SPA method in estimating the seismic demand of one-way asymmetric-plan buildings. By comparing the seismic demands predicted by different pushover analysis methods and the nonlinear response time history analysis (NLRHA) method as well as the deviations of the predicted demands, it is found that the SPA method is capable of predicting the seismic demand of singly symmetric buildings effectively and accurately, especially the heavy side, where the seismic demand is more significant.

2 Governing equation of motion for a singly symmetric building

Consider a singly symmetric building with a symmetric plan along x-axis but asymmetric plan along the y-axis. When the structure is subjected to horizontal ground motion excitations in the y-direction, $\ddot{u}_{gy}(t)$, the equation of motion can be expressed by (Chopra 2012)

$$\begin{bmatrix} \mathbf{m} & \mathbf{0} \\ \mathbf{0} & \mathbf{I_0} \end{bmatrix} \begin{Bmatrix} \ddot{\mathbf{u}}_\mathbf{y} \\ \ddot{\mathbf{u}}_\theta \end{Bmatrix} + \begin{bmatrix} \mathbf{k_{yy}} & \mathbf{k_{y\theta}} \\ \mathbf{k_{\theta y}} & \mathbf{k_{\theta\theta}} \end{bmatrix} \begin{Bmatrix} \mathbf{u_y} \\ \mathbf{u_\theta} \end{Bmatrix} = - \begin{bmatrix} \mathbf{m} & \mathbf{0} \\ \mathbf{0} & \mathbf{I_0} \end{bmatrix} \begin{Bmatrix} \mathbf{1} \\ \mathbf{0} \end{Bmatrix} \ddot{u}_{gy}(t) = - \begin{Bmatrix} \mathbf{m1} \\ \mathbf{0} \end{Bmatrix} \ddot{u}_{gy}(t) = -s\ddot{u}_{gy}(t) \tag{1}$$

where $\mathbf{m}$ is the mass matrix that is a diagonal one, with $m_{jj} = m_j$, where m_j is the lumped mass on the jth floor; $\mathbf{I}_0$ is the diagonal polar moment of inertia matrix with $I_{jj} = I_{Oj}$, where I_{Oj} is the polar moment of inertia of jth floor diaphragm on the vertical axis through the mass centre (CM); $\ddot{\mathbf{u}}_y$ and $\ddot{\mathbf{u}}_\theta$ are acceleration vectors, which are the y-lateral and torsional floor accelerations, respectively; $\mathbf{u}_y$ and $\mathbf{u}_\theta$ are the displacement vectors, whose elements are the y-lateral and torsional floor displacements, respectively; $\mathbf{k_{yy}}$, $\mathbf{k_{y\theta}}$, $\mathbf{k_{\theta y}}$ and $\mathbf{k_{\theta\theta}}$ are sub-matrices of the overall stiffness matrix of the structure; $\mathbf{s}\ddot{u}_{gy}(t)$ represents the effective earthquake forces; $\mathbf{s}$ is height-wise distribution of the effective force, and can be expressed as the sum of the modal inertia force, $\mathbf{s_n}$,

$$\mathbf{s} = \begin{Bmatrix} \mathbf{m1} \\ \mathbf{0} \end{Bmatrix} = \sum_{n=1}^{2N} \mathbf{s_n} = \sum_{n=1}^{2N} \Gamma_n \begin{Bmatrix} \mathbf{m}\phi_{yn} \\ r^2\mathbf{m}\phi_{\theta n} \end{Bmatrix} \tag{2}$$

where ϕ_{yn} and $\phi_{\theta n}$ are the lateral and rotational components of the nth natural vibration mode $\Phi_\mathbf{n}$ respectively, and the modal participating factor, Γ_n, can be calculated by

$$\Gamma_n = \frac{L_n}{M_n} \tag{3}$$

where

$$L_n = \begin{Bmatrix} \phi_{yn}^T & \phi_{\theta n}^T \end{Bmatrix} \begin{Bmatrix} \mathbf{m1} \\ \mathbf{0} \end{Bmatrix} = \phi_{yn}^T \mathbf{m1} = \sum_{j=1}^{N} m_j \phi_{jyn} \tag{4}$$

$$M_n = \begin{Bmatrix} \phi_{yn}^T & \phi_{\theta n}^T \end{Bmatrix} \begin{bmatrix} \mathbf{m} & \mathbf{0} \\ \mathbf{0} & \mathbf{I_0} \end{bmatrix} \begin{Bmatrix} \phi_{yn} \\ \phi_{\theta n} \end{Bmatrix} = \phi_{yn}^T \mathbf{m} \phi_{yn} + \phi_{\theta n}^T \mathbf{I_0} \phi_{\theta n} = \sum_{j=1}^{N} m\phi_{jyn}^2 + \sum_{j=1}^{N} I_{0j}\phi_{j\theta n}^2 \tag{5}$$

Since all the modes of vibration are independent in the elastic vibration of structures, the floor displacements of nth mode can be expressed as

$$\mathbf{u}_n = \phi_n q_n(t) = \phi_n \Gamma_n D_n(t) \tag{6}$$

Substituting Eq. (6) into Eq. (1), the equation of motion for a multi-degree-of-freedom system is converted into equations of motion of a series single-degree of freedom system, which can be solved independently. When the structure yields, the lateral force is dependent on the loading history, which can be expressed by

$$\mathbf{F}_s = \mathbf{F}_s(\mathbf{u}, t) \tag{7}$$

Thus, the governing equation of motion for the nonlinear system can be written as

$$\mathbf{m\ddot{u}} + \mathbf{c\dot{u}} + \mathbf{f}_s(\mathbf{u}, \text{sign}\mathbf{\dot{u}}) = -\mathbf{mi}\ddot{u}_g(t) \tag{8}$$

3 Development of SPA for singly symmetric buildings

For simplifying the effect of mode coupling in structural nonlinear vibration, it is assumed in the SPA method that when the structure vibrates with the *i*th mode, top displacements induced by all the prior vibration modes have reached expected values and the structural conditions, such as the forces and storey displacements of *i*th mode, will stay unvaried when the *i*th mode induced top displacement arrives at the expected value (Liu and Kuang 2017). The consecutive pushover technique, which consecutively performs some pushover analysis procedures using mode-shape distributed forces to structures to have the expected top displacement, is used to calculate the structural seismic demand. The order of the modal pushover analysis is from the fundamental mode to higher modes.

In the problem of singly symmetric structures, the first five vibration modes that have a non-zero effective modal participating mass ratio in the direction of the input motions are included. The effective modal participating mass ratio is computed by

$$\lambda_n = \frac{m_{eff}}{\sum_{i=1}^{N} m_j} = \frac{1}{\sum_{i=1}^{N} m_j} \frac{L_n^2}{M_n} \tag{9}$$

where $\sum_{i=1}^{N} m_j$ is the structural seismic mass.

The overall displacement of the roof in the direction of the input motion u_{yr0} and the target roof displacement in the y-direction u_{yir} for each pushover analysis can be obtained as

$$u_{yr0} \approx \left(\sum_{i=1}^{N} \left(\beta_i |\Gamma_i| \phi_{yir} D_i \right)^2 \right)^{0.5} \tag{10}$$

where

$$u_{yir} = \alpha_{yi} \times u_{yr0} \tag{11}$$

and D_i is the spectrum displacement values of *i*th mode; β_i is the roof displacement reduction factor; α_{yi} stands for the contribution factor of the displacement of the roof for *i*th mode in the y-direction. The reduction facto i can be calculated by

$$\beta_{\mathrm{i}} \approx \left\{ \begin{array}{c} 1.0(i = 2, 3, \ldots, N) \\ \cos(\omega_1 \times t_{N-1}) = \cos\left[\omega_1 \left(\frac{-\pi}{2\times\omega_{N-1}}\right)\right](i = 1) \end{array} \right\} \tag{12}$$

where ω_1 and $\omega_{\mathrm{N}-1}$ are the vibration frequency of the first mode and $(N-1)$th mode respectively; $t_{\mathrm{N}-1}$ is the time point where $(N-1)$th mode should start to ensure that all the vibration modes induce the expected displacements of the roof at the same time. The *i*th mode roof displacement contribution factor can be computed by

$$\alpha_{yi} = \frac{\beta_i \left| \Gamma_i \right| \phi_{yir} D_i}{\sum_{i=1}^{N} \beta_i \left| \Gamma_i \right| \phi_{yir} D_i} \tag{13}$$

Detailed steps of the SPA procedure for singly symmetric structures are summarised as follows.

1. Calculate structural seismic mass and then gravity loading for the structure.
2. Carry out eigenvalue analysis:
   a. Calculate the dynamic properties of the structure.
   b. Mode-shapes of the included modes are normalised to ensure that the component at roof ϕ_{yir} is equal to 1.
3. Compute the total roof displacement, u_{yr0}, and the target displacements of the roof for different modes, u_{yir}. Displacements of the roof are computed using Eqs. (10) and (11), where the spectrum displacement values can be obtained from the elastic design spectrum of the studied sites or the mean response spectrum of a set of ground motions.
4. Conduct the spectrum-based pushover analysis:
   a. Perform the pushover analysis with lateral force with the distribution of $s_1^* = m\phi_1$, and the structure is loaded until the roof displacement reaches u_{y1r}; then obtain the peak value of the demand r_1.
   b. With the initial structural condition that is the same as that at the last step of the previous pushover analysis procedure, carry out pushover analysis using the lateral force with the distribution of $s_2^* = m\phi_2$, until the displacement increment at the roof is equal to u_{y2r}. Then obtain the peak value of the demand r_2.
   c. Repeat Step 4b for all the modes considered with the corresponding force distribution $s_i^* = m\phi_i$, and the initial structural condition the same as that at end of last step. The *i*th analysis procedure shall stop when the roof displacement of that procedure reaches the target displacement u_{yir}; then obtain the peak demand r_i.
5. Get the maximum demand of the peak demands of all the modes considered as the demands estimated by the SPA method,

$$r = \max\left\{r_1, r_2, \ldots, r_n\right\} \tag{14}$$

Table 1 Design factors of target spectrum

Spectrum number	S_{ds} (g)	S_{d1} (g)	T_L (s)
1	1.00	0.75	12
2	1.20	0.85	10
3	1.52	0.82	12

Fig. 1 Selected elastic design spectra

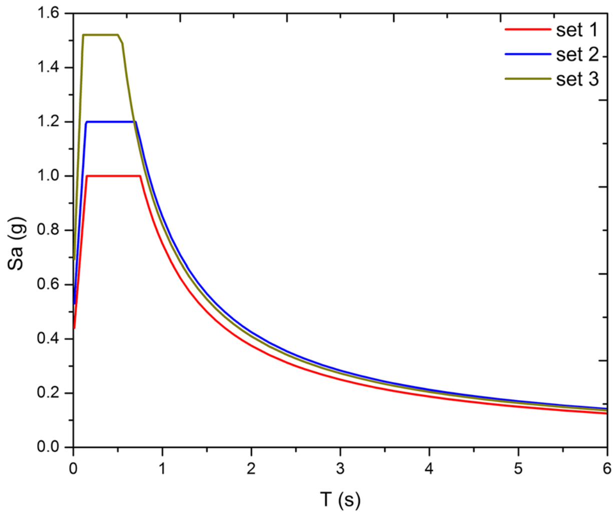

4 Verification of proposed analysis procedure

4.1 Selection of ground motions

The target spectra used for the selection and scaling of motions are three elastic design spectra (ASCE 2013) with various design parameters, which were tabulated in Table 1. The elastic acceleration design spectra are shown in Fig. 1. Three ground motion sets, with 20 motions in each set, are chosen from the PEER ground motion database and scaled up to fit the mean response spectra of the ground motions with the chosen design spectra. All the chosen motions were generated by earthquake events with a moment magnitude from 6.5 to 9.0. The distances from the stations where ground motions were recorded to the epicentre were at least 12 km and the soil type of the record station is class C of the NEHRP site. The response spectra of ground motion and the target design spectra are presented in Fig. 2. Details of the ground motions including the earthquake event, moment magnitude and recorded stations are presented in the appendix.

4.2 Prototype structures

In this verification study, two prototype structures that are a 9-storey and a 20-storey steel rigid frames denoted as F1 and F2 respectively, as shown in Figs. 3 and 4, were investigated. These frame structures were modified from the SAC frames that were originally designed for the Los Angeles, California region, with a design peak ground acceleration of 0.4 g (Ohtori et al. 2004). To involve the torsional effects, the buildings with symmetric plan arrangements were modified by keeping the stiffness property of the structure unchanged and shifting the centre of mass (CM) of each storey along the *x*-direction. In each frame series, there were three frames and the eccentricity between CM and centre of stiffness (CS), denoted as ε, for the three frames is set to be 10%, 20% and 30% of the plan dimension respectively. The moment of inertia of floors to mass ratio of floors

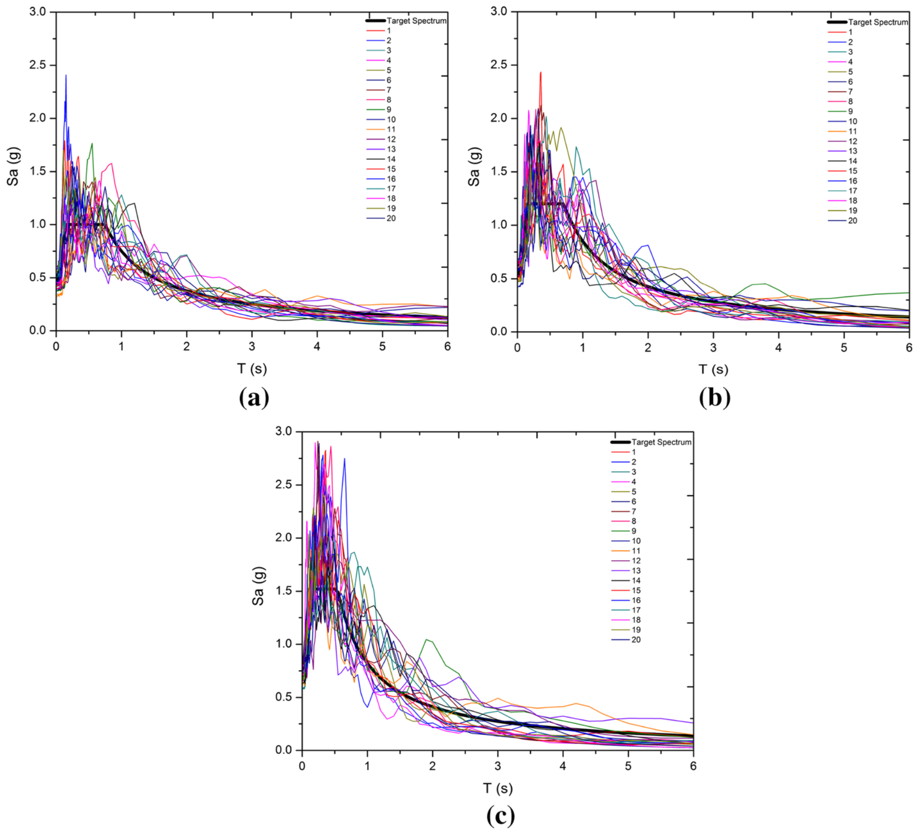

Fig. 2 Acceleration response spectra of design spectra and corresponding selected and scaled motions: **a** motion Set-1; **b** motion Set-2; **c** motion Set-3

of the one-way asymmetric structures was assumed to be equal to that of the structures with a symmetric plan to ensure that the difference in the structural behaviour of buildings with the same height is mainly caused by ε. The modified plan arrangements of the frame structures are plotted in Fig. 5. The modal properties of the first five modes with non-zero modal mass participating factors in y-direct of the frames are summarised in Table 2. Discretised hinges located at the ends of frame members are used to model the nonlinear behaviour. hinges at columns are modelled with the interaction of the axial force and bending moment, and the hinges at beams just include the effect of the bending moment. A generalised force–deformation plot is presented in Fig. 6, where Q and Q_y are the generalised force and the yield strength of the component respectively; Δ and θ represent the deformation and a, b and c are modelling parameters of the hinge. All the hinges are modelled following FEMA 365 (FEMA 2000).

4.3 Methods of analysis

A comparative case study was conducted to investigate seismic demands of the six singly symmetric frame buildings using SPA, CMP, MPA and NLRHA methods. The NLRHA

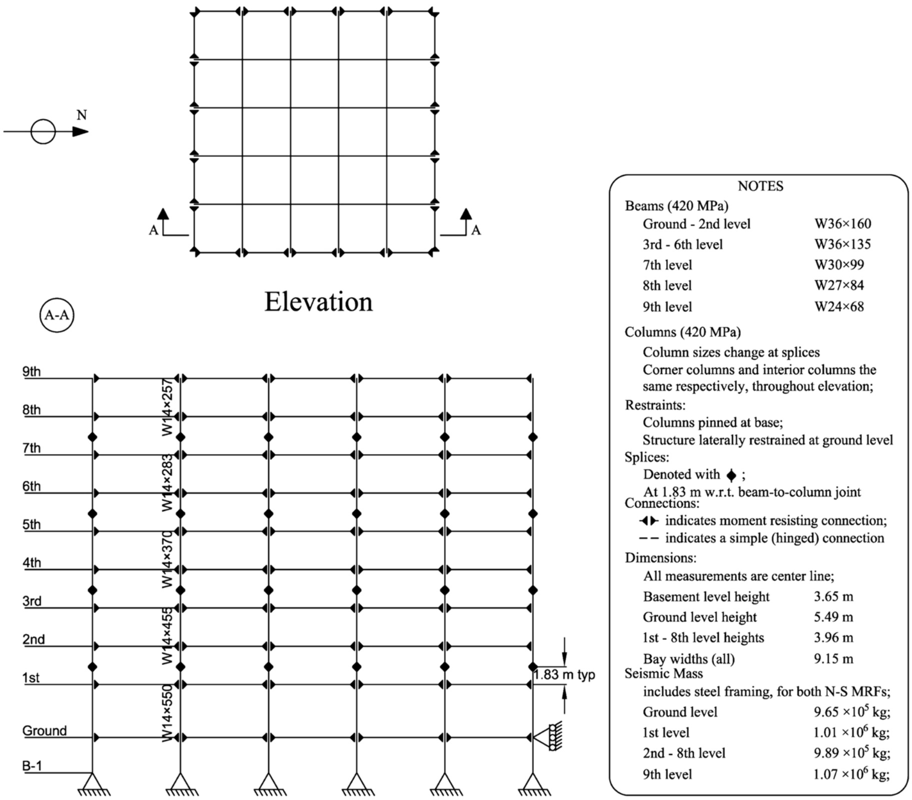

Fig. 3 Prototype frame structure F1

method with Wilson-θ time integration technique and the value of θ taken as 1.4 for the convergence of the algorithm was performed with all the chosen ground motions. The average seismic demand of NLRHA for each motion set was treated as a benchmark for comparison. The damping ratio of the first and third vibration modes was taken as 5% to construct the Rayleigh damping matrix. Similar to NLRHA, the MPA method was conducted for all the motions and the average demand was used for the comparison, where the initial three and five modes with a positive effective-modal-participating-mass ratio in the direction of the input ground motion were considered for the 9-storey frames and the 20-storey frames respectively. The CMP method was carried out with the three- stage-analysis procedure, whose target roof displacement is the mean roof displacement in the *y*-direction of NLRHA, while the SPA method was implemented following the steps given in Sect. 3. All the analytical models included the P-Δ effects, and all the analysis procedures were performed with the nonlinear version of SAP 2000 (CSI 2011).

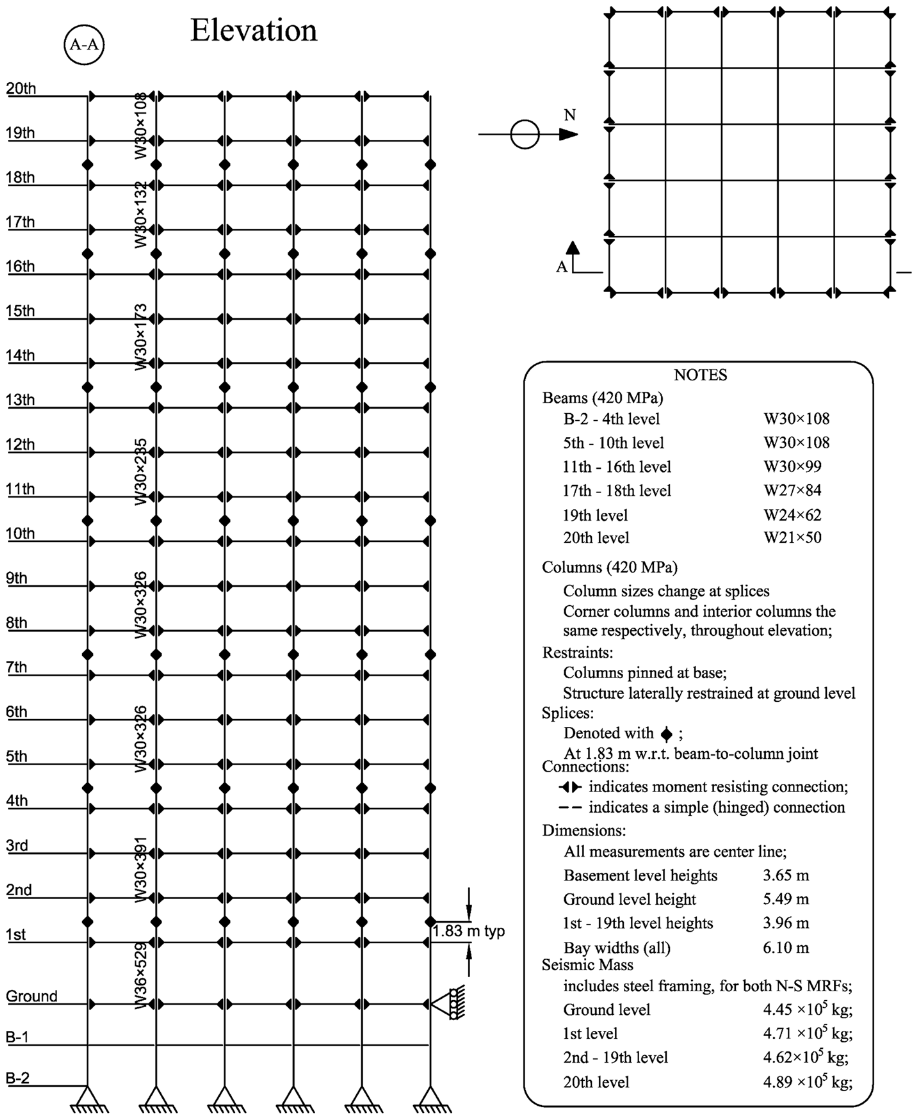

Fig. 4 Prototype frame structure F2

5 Results and discussion

Since the structures have an asymmetric plan, two sides of the frames will undergo different deformations. The side that is closer to CM will take more gravity loads than the side that is far from CM. In this study, the side that is closer to CM is denoted as the heave side (HS) and the other as the light side (LS). The relations between CM, LS and HS are given Fig. 5. The peak inters-storey drift ratios and hinge plastic-rotations on both LS and HS of F1-20 and F2-20, which are subjected to ground motions in motion Set 2, are presented in Figs. 7, 8. From a previous study (Liu and Kuang 2017), it is revealed that the mean

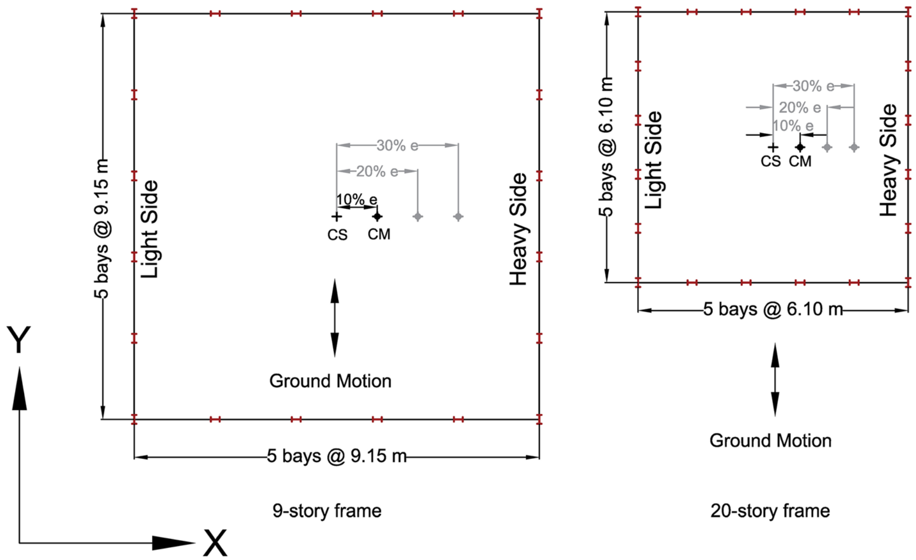

Fig. 5 Plan arrangements of frame structures

Table 2 Dynamic properties of frames used in the analysis

Frame no./storey	ε (%)	Period (s)									
		T_1	λ_1	T_2	λ_2	T_3	λ_3	T_4	λ_4	T_5	λ_5
F1-10/9	10	2.292	0.730	1.796	0.084	0.853	0.100	0.674	0.012	0.489	0.036
F1-20/9	20	2.446	0.660	1.686	0.150	0.911	0.090	0.632	0.021	0.524	0.033
F1-30/9	30	2.635	0.640	1.570	0.180	0.982	0.088	0.588	0.019	0.564	0.038
F2-10/20	10	3.394	0.690	2.589	0.056	1.178	0.095	0.920	0.010	0.693	0.031
F2-20/20	20	3.599	0.630	2.443	0.120	1.255	0.086	0.865	0.019	0.741	0.028
F2-30/20	30	3.860	0.610	2.284	0.140	1.349	0.084	0.808	0.017	0.798	0.033

Fig. 6 Force-deformation modelling of hinges

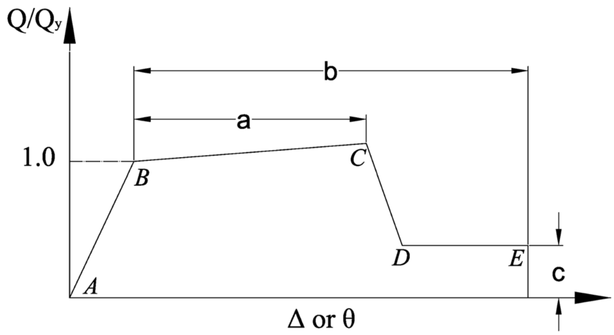

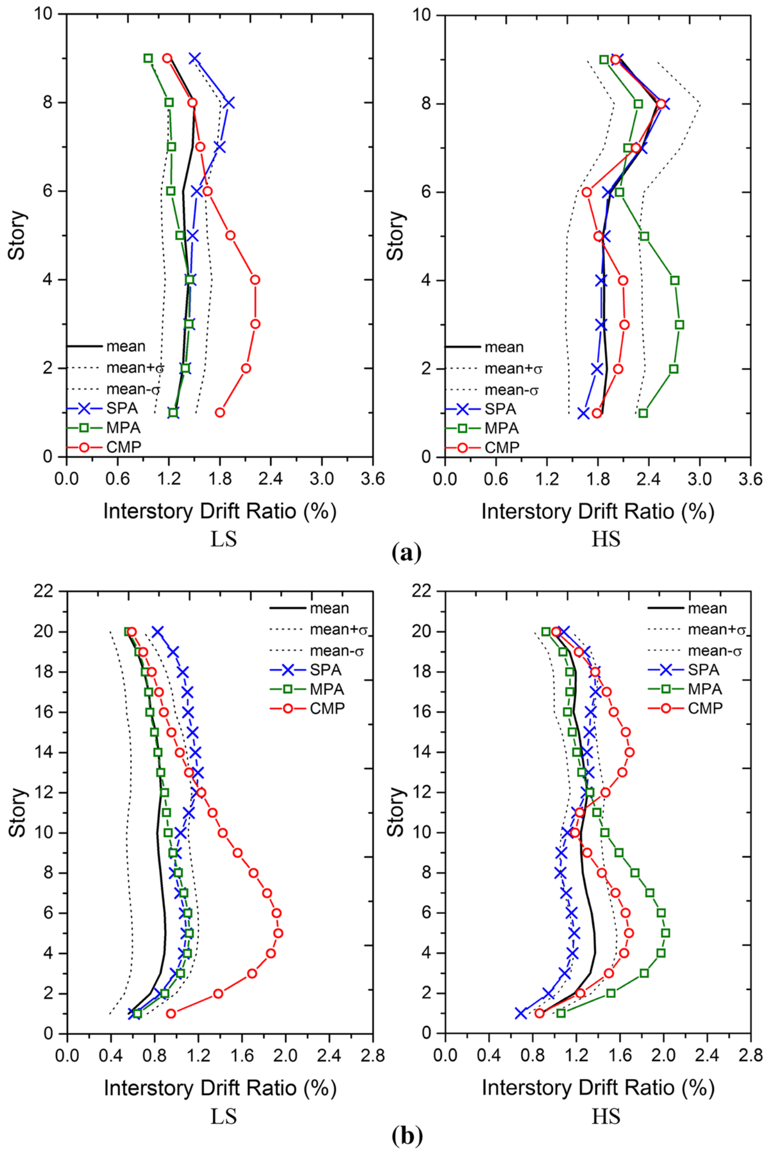

Fig. 7 Comparison of the inter-story drift ratio of frame structures subjected to ground motion Set 2: **a** F1-20; **b** F2-20

demand ± one standard deviation, σ, of the demands of the whole set (one deviation range) calculated by NLRHA is a very good tool for assessing the reasonability of the results by the pushover analysis methods. Hence, the mean demand plus and minus σ is also plotted and denoted as MEAN + σ and MEAN-σ, as shown in Figs. 7, 8.

Figure 7 presents the inter-storey drift ratio of F1-20 and F2-20 that were subjected to the ground motions in ground motion Set 2. As for the inter-story drift ratio of LS of F1-20, it is seen that SPA predicted the drift ratio on LS best from the bottom to

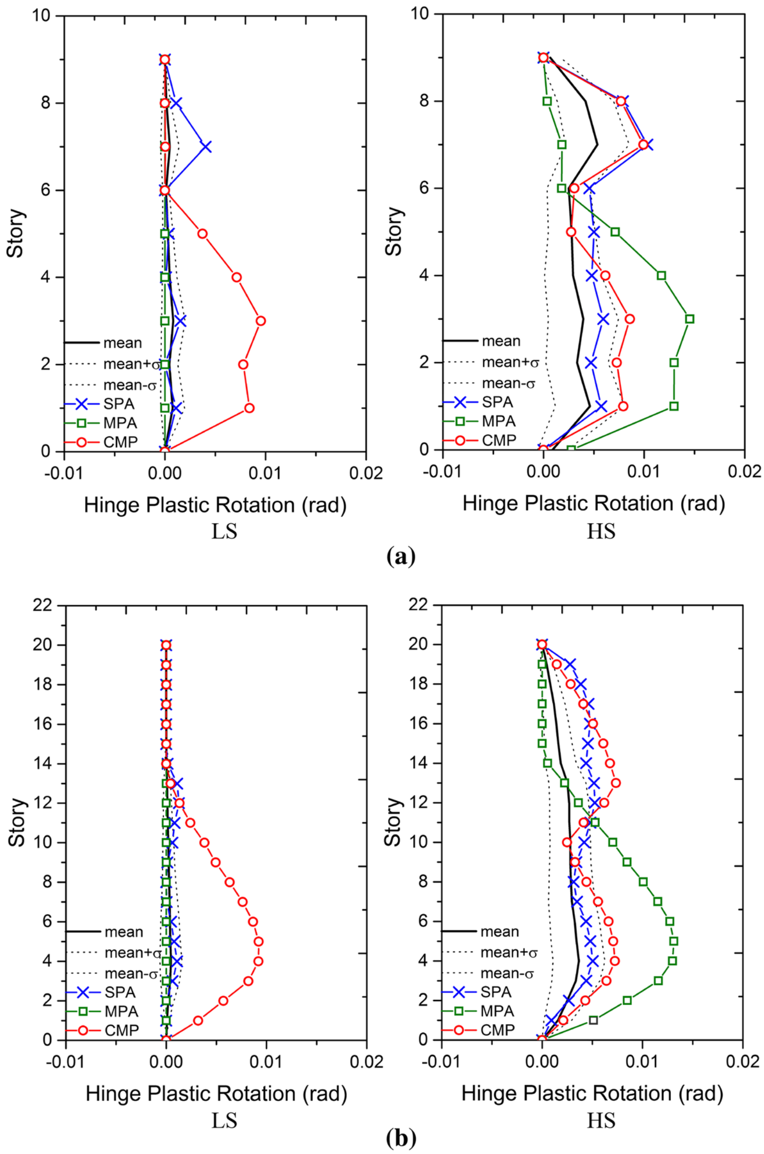

Fig. 8 Comparison of the hinge plastic rotation of frame structures subjected to ground motion Set 2: **a** F1-20; **b** F2-20

6th storey, and conservatively estimated the drift ratio at upper storeys, while the MPA method predicted the drift ratio at the lower part well, but underestimated the drift ratio at the upper part. Although the CMP method estimated the drift ratio well at the top, it overpredicted the drift ratio significantly at the lower part of the structure. The distribution of the inter-storey drift ratio of LS of F2-20 in Fig. 6b, where, it is found that MPA predicted the drift ratio best since all the results are within the range of one deviation and the prediction matches the mean drift ratio of NLRHA very well. SPA gave the good predictions for the drift ratio until the storey reaches the 10th level, then the drift ratios predicted by SPA become slightly conservative as compared with those of NLRHA. The drift ratio predicted by CMP method at lower storeys is considerably larger than that of the mean drift ratio of NLRHA.

As for the inter-story drift ratio of HS of F1-20 under the action of ground motions from motion Set 2, it can be seen from Fig. 7a that SPA was capable of predicting the drift ratio on HS of the F1-20 structure best, since the drift ratio of SPA fits the best with the mean result of NLRHA and all the results are within the range of one deviation. Although most of the drift ratios of CMP is within the one deviation range, CMP method was prone to overestimating the drift ratios at 1-4 storeys. The MPA method predicted the drift ratio well at upper levels of the 9-storey frames but overestimated the drift ratio at lower storeys considerably. When comparing the inter-storey drift ratios on HS of the F2-20, it is seen that SPA still can predict the mean drift ratio best and all the results are within the range of one deviation. While CMP overestimated the drift ratios at both lower and upper storeys and underestimated the drift ratios at the middle part of F2-20. MPA estimated the drift ratio at upper storeys well but provided much conservative prediction at the lower storeys.

The distribution of the peak hinge plastic-rotation on LS and HS of F1-20 and F2-20 when using the ground motions from motion Set 2 as the input motions is plotted in Fig. 8. It is seen from Fig. 8 that there is a significant difference between the hinge plastic rotation in the HS and LS of the structures. The plastic-rotation on the LS of both structures approaches gradually to zero, but the hinge plastic rotation on the HS is much more significant compared with that in LS. The very small hinge plastic-rotation indicates that the plastic deformation of frame members on LS is minor. By comparing the hinge plastic-rotations computed by the pushover methods, SPA and MPA had a rational estimate of the plastic-rotation on LS, although the results from SPA are slightly conservative at upper floors of F1-20, while CMP overestimated the rotation significantly at the lower storeys for both structures.

For the comparison of the hinge plastic-rotations on the HS of F1-20 and F2-20 predicted by the different pushover methods and NLRHA, it is seen that SPA estimated the plastic rotation of hinges best from the bottom to about two-thirds of the height of structures, where MPA and CMP over-predicted considerably the hinge plastic-rotation. When the hinge plastic-rotations of the upper part of the structure occur, there are obvious variations between the results from the pushover methods and those from NLRHA. This is because both SPA and CMP over-predicted the plastic-rotation of hinges, while MPA provided a reasonable prediction for the hinge plastic-rotation. However, it can be seen that most of the hinge plastic-rotations predicted by MPA and CMP are not within the one deviation range, while most results of SPA are within the range of one deviation. Thus, the SPA method can estimate the hinge plastic-rotations well.

To quantitatively judge the accuracy and reasonability of the results predicted by the pushover analysis methods, the deviation between the predictions from the pushover analysis methods and that of the NLRHA method is compared. The deviations are computed as

$$D_{i,j,k,N} = \frac{\left| d_{i,j,k,N} - \bar{d}_{i,j,k} \right|}{\sigma_{i,j,k}} \tag{14}$$

where, $D_{i,j,k,N}$ is the deviation of pushover analysis method N, $d_{i,j,k,N}$ is the seismic demand estimated by pushover analysis procedure N, $\bar{d}_{i,j,k}$ is the mean seismic demand computed by the NLRHA method and $\sigma_{i,j,k}$ represents the standard deviation of the seismic demand of NLRHA method of the whole set, with respect to the results for ith level of jth structure when subjected to ground motions from motion Set k. There are two reasons for replacing the benchmark results $\bar{d}_{i,j,k}$ by $\sigma_{i,j,k}$ to serve as the denominator when computing the deviations. Firstly, the hinge plastic rotation of LS computed by NLRHA is so small that the value approaches zero, using a number that is close to zero as the denominator will induce an unreasonably large value. The unreasonably large value of deviation will cause troubles to the comparison. Meanwhile, the standard deviation $\sigma_{i,j,k}$ has a larger value comparing to that of the mean hinge plastic rotation of LS of the structures. At the same time, the value of $\sigma_{i,j,k}$ of other demands has a similar order of magnitude to that of the mean values of the corresponding demands. Secondly, the deviation computed following the Eq. (14) reveal the relations between the difference of the results of the pushover analysis and NLRHA method and the standard deviation. If the $D_{i,j,k,N}$ is smaller than one, the difference between the results of the pushover analysis and NLRHA method is smaller than the standard deviation and the results of the pushover analysis method N is within the one standard deviation range. Consequently, the deviation $D_{i,j,k,N}$ can clearly quantify the accuracy as well as the reasonability of the estimation of the pushover analysis methods.

Plotted in Figs. 9 and 10 are the statistics of the deviations of inter-storey drift ratio and hinge plastic rotation respectively when using pushover analysis methods to predict the

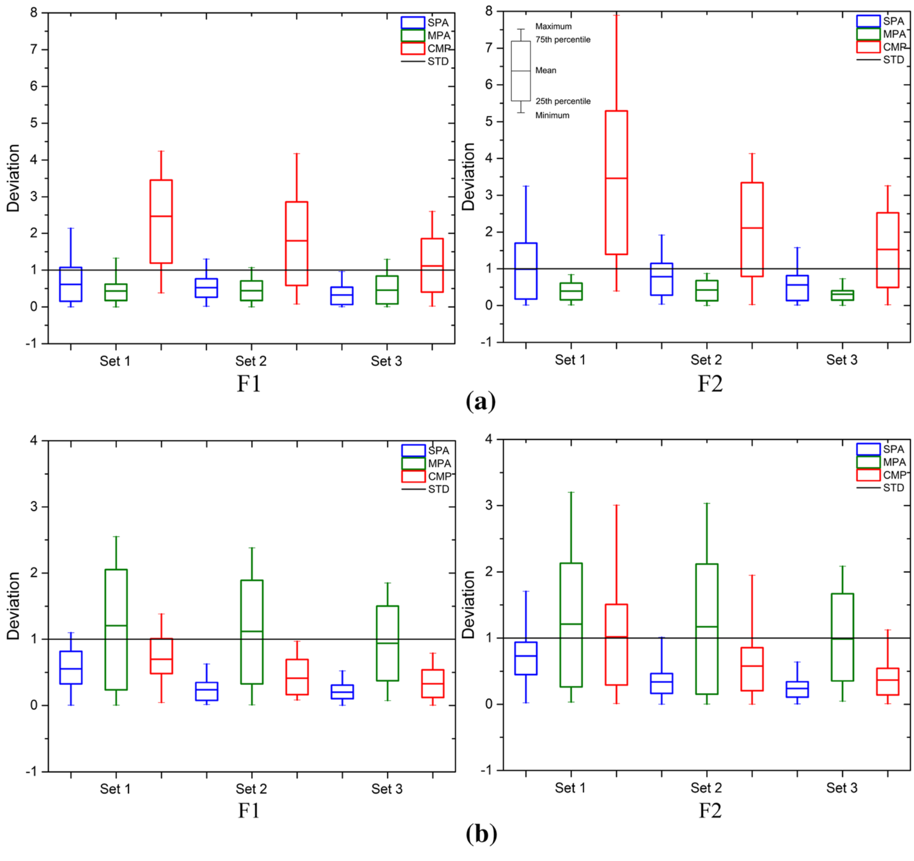

Fig. 9 Deviation of the prediction inter-story drift ratio: **a** LS; **b** HS

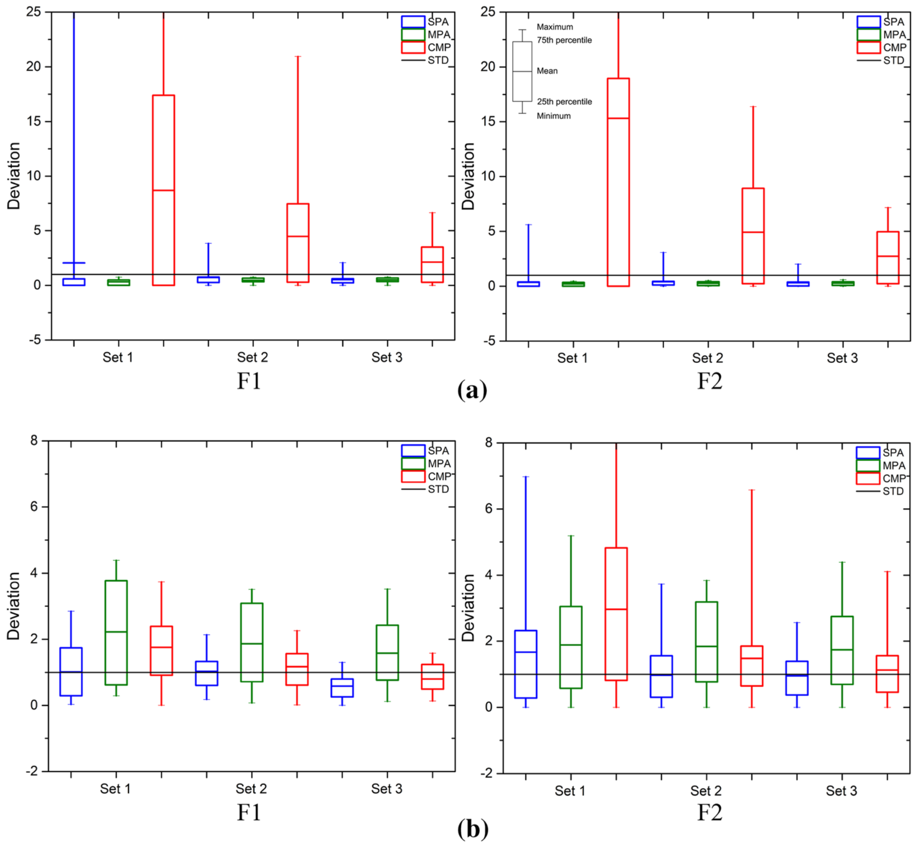

Fig. 10 Deviation of the prediction hinge plastic rotation: **a** LS; **b** HS

seismic demands of all the frame structures under all the three sets of selected motions. For each box plot, values of the top and bottom whiskers represent the maximum and minimum deviation respectively, and the values of top and bottom edges of the box stand for the deviation values with 75th and 25th percentiles respectively. From Fig. 9a, where the deviation of the inter-story drift ratio at LS of the structures is presented, it is found that the mean deviation of MPA is the smallest and the highest deviation of the MPA is close to one. Except for the case where the 20-storey frames under motion Set 1, most of the deviations of SPA method are less than one, since the deviation value with 75th percentile is not more than one. But for the CMP method, whose average deviation is the largest among that of the pushover analysis methods, the deviation with 25th percentile is close to one, indicating that most of the deviations of the CMP method have values greater than one. While for the deviation of the prediction of the inter-storey drift ratio at the HS, it is seen from Fig. 9b that the SPA method has the lowest mean deviation and the maximum deviation of the results of the SPA method is less than one except for motion Set 1, where the maximum deviation of the SPA is marginally over one. The mean deviation, as well as deviation value of 75th percentile of the CMP, is smaller than the corresponding value of the MPA method.

Thus, from the comparison of the deviation of the inter-storey drift ratio, it is found that the MPA can predict the drift ratio at LS the best since the deviation is the minimum and almost all the predictions are with one standard deviation range, but the prediction of the MPA method on the inter-storey drift ratio of HS of structure is not satisfactory. The CMP method can reasonably estimate the drift ratio at the HS, because most of the deviation is below one, meaning that most of the predictions of the CMP method located in the one standard deviation range. However, the CMP method cannot predict the drift ratio at the LS well. Among the pushover analysis methods, only the SPA method can reasonably predict the drift ratio at both LS and HS of the structures, since the majority of the deviations of SPA are beneath one. Besides, the SPA is also capable of providing the best predictions of the drift ratio at the HS of the structure.

In Fig. 10a, where the deviations of the hinge plastic rotation of the LS of structures is presented, it is still the MPA that has the slightest maximum deviations among the three methods, and all the maximum deviations are less the one. As for deviation of SPA method, although the peak deviation of the F1 structures is very large, when the structure is subjected to motions from motion Set 1, the values of deviation of 75th percentile are all not more than one, implying that the majority of the deviations of the hinge plastic rotation of LS computed from the SPA method is below one. While the deviations of the CMP method are very noticeable with the deviation of a 75th percentile reaching just below 20. The deviation of the hinge plastic rotation of the HS is shown in Fig. 10b, where it is noted that the mean deviation, as well as the deviation for 75th percentile of the SPA method, is the lowest among the pushover analysis methods, which shows that the deviation of the hinge plastic rotation of SPA method is much less significant, compared with the other two methods. Comparing the deviation of the CMP and MPA methods, it can be found that the CMP method has a less significant deviation, with slighter mean deviation and smaller deviation for the 75th percentile.

Resulting from the comparison of the deviation of the hinge plastic rotation, it is noted that both MPA and SPA method can reasonably predict the hinge plastic rotation, as the mean deviation as well as the deviations with 75th percentile of the two methods are small and close to one. The MPA predicted the hinge plastic rotation at the LS better while the SPA estimated the hinge plastic rotation at the HS better. Taking the advantage that the hinge plastic rotation of HS is much more significant, SPA is a better choice for the prediction of the hinge plastic rotation.

6 Conclusions

The spectrum-based pushover analysis (SPA) procedure is expanded to estimate the seismic demands of singly symmetric buildings. The simplification of the mode coupling in the nonlinear vibration of structures proposed in the SPA method for a symmetric structure is adopted in the analysis. Using the forces with mode shape distributions, including the translation and rotation components, the torsional issues caused by one-way structural asymmetry is considered. A case study for two series of steel buildings, which are tall ridged frame structures with different storey numbers and mass centre eccentricities under various levels of input motions, was conducted. Different advanced pushover analysis methods and the most rigorous nonlinear response time history analysis (NLRHA) were used to conduct the analysis and compute the seismic demands of the singly symmetric frame structures. Based on the comparison of the seismic demands, the conclusions are drawn as follows.

1. Among the three pushover analysis methods, only the SPA procedure can reasonably predict the seismically induced deformation, including both inter-storey drift ratio and hinge plastic rotation, since the majority of the differences between the results of the SPA method and the NLRHA method are less than the standard deviation of the seismic demand of the NLRHA method and most of the seismic demands from the SPA procedure are within one standard deviation range.
2. For the seismic demands on the heavy side (HS) of the structures, which is more important for the cases in connection to the torsional effect of buildings, the proposed SPA method estimates both inter-storey drift ratios and hinge plastic-rotations the best among all the advanced pushover analysis methods. The results of the seismic demands show very good agreement with those predicted by NLRHA, while CMP and MPA cannot predict the seismic demands at the lower part of the structures well.
3. On the light side (LS) of the structures, which is farther from the centre of mass, the SPA method can provide reasonably good estimations of the seismic demands, although the MPA method predicted the seismic demands the best. The CMP method overestimated significantly the demands in the lower part of the structures but has good results in the upper part.
4. Owing to the nature of design spectrum-based computations and its efficiency, yet accuracy, the proposed SPA procedure is considered as one of the most promising tools for quickly estimating the seismic demands of singly symmetric-plan buildings.

Acknowledgements The study was supported in part by the Research Grants Council of Hong Kong under Grant Number 16209115.

Appendix

See Tables 3, 4 and 5.

Table 3 Information of ground motions in motion Set 1

Record id	Scale factor	Earthquake name	Year	Station name	Magnitude	Component (deg)
1	4.764	Loma Prieta	1989	Fremont—Mission San Jose	6.93	0
2	4.582	Loma Prieta	1989	Gilroy Array #6	6.93	0
3	2.303	Loma Prieta	1989	Palo Alto—SLAC Lab	6.93	270
4	3.548	Cape Mendocino	1992	Fortuna—Fortuna Blvd	7.01	0
5	4.805	Chi-Chi_Taiwan	1999	HWA009	7.62	E
6	4.790	Chi-Chi_Taiwan	1999	HWA012	7.62	E
7	4.415	Chi-Chi_Taiwan	1999	HWA028	7.62	E
8	4.663	Chi-Chi_Taiwan	1999	HWA029	7.62	E
9	4.332	Chi-Chi_Taiwan	1999	HWA055	7.62	N
10	2.098	Chi-Chi_Taiwan	1999	TCU042	7.62	E
11	2.348	Chi-Chi_Taiwan	1999	TCU061	7.62	E
12	4.396	Chi-Chi_Taiwan	1999	TCU092	7.62	E
13	2.326	Hector Mine	1999	Amboy	7.13	90
14	3.832	Hector Mine	1999	Joshua Tree	7.13	90
15	1.133	Cape Mendocino	1992	Ferndale Fire Station	7.01	70
16	3.021	Cape Mendocino	1992	"South Bay Union School"	7.01	270
17	3.642	Landers	1992	North Palm Springs Fire Sta #36	7.28	90
18	4.190	Chuetsu-oki_Japan	2007	Tokamachi Matsunoyama	6.80	NS
19	3.803	Chuetsu-oki_Japan	2007	Sawa Mizuguti Tokamachi	6.80	NS
20	3.756	Darfield_New Zealand	2010	WAKC	7.00	E

Table 4 Information of ground motions in motion Set 2

Record id	Scale factor	Earthquake name	Year	Station name	Magnitude	Component (deg)
1	4.106	Kern County	1952	Taft Lincoln School	7.36	21
2	3.828	Irpinia_Italy-01	1980	"Calitri	6.9	0
3	4.319	Loma Prieta	1989	APEEL 7—Pulgas	6.93	0
4	3.975	Loma Prieta	1989	Coyote Lake Dam—Southwest Abutment	6.93	195
5	4.168	Cape Mendocino	1992	Fortuna—Fortuna Blvd	7.01	0
6	4.620	Northridge-01	1994	LA—Temple & Hope	6.69	90
7	3.888	Chi-Chi_Taiwan	1999	HWA033	7.62	E
8	4.179	Chi-Chi_Taiwan	1999	HWA051	7.62	N
9	3.610	Chi-Chi_Taiwan	1999	TCU015	7.62	E
10	2.247	Chi-Chi_Taiwan	1999	TCU116	7.62	E
11	2.619	Hector Mine	1999	Amboy	7.13	90
12	4.536	Hector Mine	1999	Joshua Tree	7.13	90
13	1.404	Cape Mendocino	1992	Ferndale Fire Station	7.01	270
14	2.127	Cape Mendocino	1992	Loleta Fire Station	7.01	270
15	3.357	Cape Mendocino	1992	South Bay Union School	7.01	270
16	4.136	Landers	1992	North Palm Springs Fire Sta #36	7.28	90
17	2.624	Chuetsu-oki_Japan	2007	Tani Kozima Nagaoka	6.80	NS
18	4.146	Chuetsu-oki_Japan	2007	Sawa Mizuguti Tokamachi	6.80	NS
19	2.729	Iwate_Japan	2008	Matsuyama City	6.90	NS
20	2.862	Iwate_Japan	2008	Yuzawa Town	6.90	NS

Table 5 Information of ground motions in motion Set 3

Record id	Scale factor	Earthquake name	Year	Station name	Magnitude	Component (deg)
1	4.765	Kern County	1952	Taft Lincoln School	7.36	21
2	4.211	Imperial Valley-06	1979	Cerro Prieto	6.53	147
3	4.565	Irpinia_Italy-01	1980	"Calitri	6.9	0
4	3.225	Loma Prieta	1989	Anderson Dam (Downstream)	6.93	250
5	4.376	Loma Prieta	1989	Coyote Lake Dam—Southwest Abutment	6.93	195
6	1.479	Northridge-01	1994	Castaic—Old Ridge Route	6.69	90
7	4.095	Northridge-01	1994	LA—Brentwood VA Hospital	6.69	195
8	4.106	Chi-Chi_Taiwan	1999	CHY010	7.62	N
9	4.569	Chi-Chi_Taiwan	1999	CHY046	7.62	E
10	4.575	Chi-Chi_Taiwan	1999	HWA033	7.62	E
11	3.377	Hector Mine	1999	Amboy	7.13	90
12	1.749	Cape Mendocino	1992	Ferndale Fire Station	7.01	270
13	2.675	Cape Mendocino	1992	Loleta Fire Station	7.01	270
14	4.153	Cape Mendocino	1992	South Bay Union School	7.01	270
15	4.539	Chuetsu-oki_Japan	2007	Joetsu Yasuzukaku Yasuzuka	6.80	NS
16	3.965	Chuetsu-oki_Japan	2007	Matsushiro Tokamachi	6.80	NS
17	2.354	Chuetsu-oki_Japan	2007	Yoshikawaku Joetsu City	6.80	NS
18	3.362	Chuetsu-oki_Japan	2007	Tokamachi Chitosecho	6.80	NS
19	2.405	Chuetsu-oki_Japan	2007	Yoitamachi Yoita Nagaoka	6.80	NS
20	3.196	Iwate_Japan	2008	Yuzawa Town	6.90	NS

References

Antoniou S, Pinho R (2004a) Advantages and limitations of adaptive and non-adaptive force-based pushover procedures. J Earthquake Eng 8:497–522

Antoniou S, Pinho R (2004b) Development and verification of a displacement-based adaptive pushover procedure. J Earthquake Eng 8:643–661

Antoniou S, Rovithakis A, Pinho R (2002) Development and verification of a fully adaptive pushover procedure. In: Proceedings of the twelfth european conference on earthquake engineering

ASCE (2013) Minimum Design Loads for Buildings and Other Structures (ASCE/SEI 7-10). American Society of Civil Engineering, Reston, Virginia

Bergami AV, Forte A, Lavorato D, Nuti C (2017) Proposal of an incremental modal pushover analysis (IMPA). Earthq Struct 13:539–549

Bhatt C, Bento R (2014) The extended adaptive capacity spectrum method for the seismic assessment of plan-asymmetric buildings. Earthq Spectra 30:683–703

Brozovič M, Dolšek M (2014) Envelope-based pushover analysis procedure for the approximate seismic response analysis of buildings. Earthq Eng Struct Dyn 43:77–96

Chopra AK (2012) Dynamics of structures: theory and applications to earthquake engineering, 4th edn. Prentice Hall, Hong Kong

Chopra AK, Goel RK (2002) A modal pushover analysis procedure for estimating seismic demands for buildings. Earthq Eng Struct Dyn 31:561–582

Chopra AK, Goel RK (2004) A modal pushover analysis procedure to estimate seismic demands for unsymmetric-plan buildings. Earthq Eng Struct Dyn 33:903–927

Chopra AK, Goel RK, Chintanapakdee C (2004) Evaluation of a modified MPA procedure assuming higher modes as elastic to estimate seismic demands. Earthq Spectra 20:757–778
CSI (2011) SAP2000 v-15.0: integrated finite element analysis and design of structures basic analysis reference manual, Computers and Structures Inc, Berkeley, California
FEMA P (2000) Commentary for the seismic rehabilitation of buildings. FEMA-356, Federal Emergency Management Agency, Washington, DC
Khoshnoudian F, Kiani M (2012) Modified consecutive modal pushover procedure for seismic investigation of one-way asymmetric-plan tall buildings. Earthq Eng Eng Vib 11:221–232
Kreslin M, Fajfar P (2012) The extended N2 method considering higher mode effects in both plan and elevation. Bull Earthq Eng 10:695–715
Liu Y, Kuang JS (2017) Spectrum-based pushover analysis for estimating seismic demand of tall buildings. Bull Earthq Eng 15:4193–4214
Ohtori Y, Christenson R, Spencer B Jr, Dyke S (2004) Benchmark control problems for seismically excited nonlinear buildings. J Eng Mech 130:366–385
Poursha M, Khoshnoudian F, Moghadam A (2009) A consecutive modal pushover procedure for estimating the seismic demands of tall buildings. Eng Struct 31:591–599
Poursha M, Khoshnoudian F, Moghadam A (2011) A consecutive modal pushover procedure for nonlinear static analysis of one-way unsymmetric-plan tall building structures. Eng Struct 33:2417–2434
Poursha M, Khoshnoudian F, Moghadam A (2014) The extended consecutive modal pushover procedure for estimating the seismic demands of two-way unsymmetric-plan tall buildings under influence of two horizontal components of ground motions. Soil Dyn Earthq Eng 63:162–173
Reyes JC, Chopra AK (2011a) Evaluation of three-dimensional modal pushover analysis for unsymmetric-plan buildings subjected to two components of ground motion. Earthq Eng Struct Dyn 40:1475–1494
Reyes JC, Chopra AK (2011b) Three-dimensional modal pushover analysis of buildings subjected to two components of ground motion, including its evaluation for tall buildings. Earthq Eng Struct Dyn 40:789–806
Shakeri K, Tarbali K, Mohebbi M (2012) An adaptive modal pushover procedure for asymmetric-plan buildings. Eng Struct 36:160–172

Publisher's Note Springer Nature remains neutral with regard to jurisdictional claims in published maps and institutional affiliations.